

Edith Cowan University
Research Online

ECU Publications Post 2013

1-1-2019

CO₂-wettability of sandstones exposed to traces of organic acids: Implications for CO₂ geo-storage

Muhammad Ali
Edith Cowan University

Muhammad Arif

Muhammad Faraz Sahito

Sarmad Al-Anssari
Edith Cowan University

Alireza Keshavarz
Edith Cowan University

See next page for additional authors

Follow this and additional works at: <https://ro.ecu.edu.au/ecuworkspost2013>

 Part of the [Geotechnical Engineering Commons](#)

[10.1016/j.ijggc.2019.02.002](https://doi.org/10.1016/j.ijggc.2019.02.002)

This is an Author's Accepted Manuscript of: Ali, M., Arif, M., Sahito, M. F., Al-Anssari, S., Keshavarz, A., Barifcani, A., . . . Iglauer, S. (2019). CO₂-wettability of sandstones exposed to traces of organic acids: Implications for CO₂ geo-storage. *International Journal of Greenhouse Gas Control*, , 61-68. Available [here](#)

© 2019. This manuscript version is made Available under the CC-BY-NC-ND 4.0 license

<http://creativecommons.org/licenses/by-nc-nd/4.0/>

This Journal Article is posted at Research Online.

<https://ro.ecu.edu.au/ecuworkspost2013/5855>

Authors

Muhammad Ali, Muhammad Arif, Muhammad Faraz Sahito, Sarmad Al-Anssari, Alireza Keshavarz, Ahmed Barifcani, Linda Stalker, Mohammad Sarmadivaleh, and Stefan Iglauer

© 2019. This manuscript version is made available under the CC-BY-NC-ND 4.0 license
<http://creativecommons.org/licenses/by-nc-nd/4.0/>



CO₂-wettability of sandstones exposed to traces of organic acids; implications for CO₂ geo-storage

Muhammad Ali^{a,b*}, Muhammad Arif^{a,c}, Muhammad Faraz Sahito^d, Sarmad Al-Ansari^{b,e},
Alireza Keshavarz^b, Ahmed Barifcani^a, Linda Stalker^f, Mohammad Sarmadivaleh^a, Stefan
Iglauer^{b,a},

^aDepartment of Petroleum Engineering, WA School of Mines: Minerals, Energy and
Chemical Engineering, Curtin University, 26 Dick Perry Avenue, 6151 Kensington,
Australia

^bSchool of Engineering, Edith Cowan University, 270 Joondalup Drive, Joondalup, WA
6027 Australia

^cDepartment of Petroleum Engineering, University of Engineering & Technology, Lahore,
Pakistan

^dDepartment of Electrical Engineering, King Fahd University of Petroleum and Minerals,
Dhahran, 31261, Saudi Arabia

^eDepartment of Chemical Engineering, College of Engineering, University of Baghdad,
Baghdad, Iraq.

^fCSIRO, 26 Dick Perry Avenue, Kensington, WA, 6151 Australia

*corresponding author: muhammad.ali7@postgrad.curtin.edu.au

Abstract

Wettability of CO₂-brine-mineral systems plays a vital role during geological CO₂-storage. Residual trapping is lower in deep saline aquifers where the CO₂ is migrating through quartz rich reservoirs but CO₂ accumulation within a three-way structural closure would have a high storage volume due to higher CO₂ saturation in hydrophobic quartz rich reservoir rock. However, such wettability is only poorly understood at realistic subsurface conditions, which

27 are anoxic or reducing. As a consequence of the reducing environment, the geological
28 formations (i.e. deep saline aquifers) contain appreciable concentrations of various organic
29 acids. We thus demonstrate here what impact traces of organic acids exposed to storage rock
30 have on their wettability. Technically, we tested hexanoic acid, lauric acid, stearic acid and
31 lignoceric acid and measured wettability as a function of organic acid concentration at realistic
32 storage conditions (i.e. 25 MPa and 323 K (50 °C)). In addition, measurements were also
33 conducted at ambient conditions in order to quantify the incremental pressure effect on
34 wettability. Clearly, the quartz surface turned significantly less water-wet with increasing
35 organic acid concentrations, even at trace concentrations. Importantly, we identified a threshold
36 concentration at $\sim 10^{-6}$ M organic acid, above which quartz wetting behaviour shifts from
37 strongly water-wet to an intermediate-wet state. This wettability shift may have important
38 consequences for CO₂ residual trapping capacities, which may be significantly lower than for
39 traditionally assumed water-wet conditions where CO₂ is migrating through quartz rich
40 reservoirs.

41

42 **1. Introduction**

43 CO₂ geological storage can significantly contribute towards a green environment via permanent
44 CO₂ immobilization in deep underground formations, e.g. deep saline aquifers and depleted
45 hydrocarbon reservoirs (Blunt et al., 1993, IPCC, 2005, Orr, 2009;). Efficient and safe CO₂
46 geological storage involves a qualitative and quantitative assessment of the contribution of the
47 different functional trapping mechanisms which prevent the buoyant CO₂ from migrating back
48 to the surface (IPCC, 2005; Juanes et al., 2010). These trapping mechanism include structural
49 trapping (Iglauer et al., 2015a, Arif et al., 2016a,b, 2017a;), capillary or residual trapping
50 (Juanes et al., 2010; Iglauer et al., 2011a,b; Pentland et al., 2011; Krevor et al., 2012), mineral
51 trapping (Gaus 2010; Golding et al., 2011; Pearce et al., 2015,) and dissolution trapping

52 (Iglauer 2011c; Agartan et al., 2015). In addition, adsorption trapping has been identified as
53 another storage mechanism functional in coal seams and organic rich shales (Busch et al., 2008;
54 Shojai Kaveh et al., 2012, 2016; Arif et al., 2016c, 2017b).

55 Structural and residual trapping are strongly influenced by the CO₂-brine-rock wettability
56 (Chaudhary et al., 2013; Iglauer et al. 2015a,b; Al-Menhali et al. 2016a,b; Rahman et al., 2016;
57 Al-Khdheawi et al., 2017; Arif et al. 2017a; Iglauer 2017; Wan et al., 2018), however,
58 wettability is a complex parameter which is not well understood, particularly for realistic
59 subsurface conditions. One key aspect of realistic subsurface conditions is their anoxic or
60 reducing character, which results in the existence of organic molecules in target storage
61 formations (Meredith et al., 2000; Watson et al. 2002).

62 It is shown in previous studies that water receding contact angle on the cap rock (i.e. CO₂
63 displacing water) is related to structural trapping (below an impermeable caprock; Broseta et
64 al., 2012). Whereas, the advancing water contact angle (water displacing CO₂) is related to
65 capillary trapping in the reservoir rock (Chiquet et al. 2007; and thus the amount of residually
66 trapped CO₂; Chaudhary et al., 2013, Rahman et al. 2016, Al-Menhali et al. 2016a). Note
67 further that dissolution trapping in the reservoir rock is significantly affected by the wettability
68 and it is thus necessary to know the wettability for accurate reservoir simulations and storage
69 capacity predictions (Al-Khdheawi et al. 2016, 2017).

70 Although the concentrations of organic molecules in deep aquifers is normally low (Stalker et
71 al. 2013), their prevailing concentrations are potentially sufficient to significantly influence the
72 rock's wettability characteristics (Standnes and Austad, 2003; Gomari et al., 2006; Iglauer et
73 al., 2014). Indeed, a partial mono-molecular layer adsorbed to the mineral surface would be
74 sufficient for this (Shafrin et al., 1962; Gaines 1966; Kuhn et al., 1971; Zasadzinski et al., 1994;
75 Adamson and Gast 1997; Maboudian et al., 1997; Bikkina 2011; Mahadevan 2012).

76 These minute organic concentrations can adversely affect the storage capacities and
77 containment security via their impact on CO₂ wettability (Iglauer et al. 2015a,b; Al-Khdheawi
78 et al. 2016, 2017). It is therefore important to understand at what organic concentration the
79 impact on CO₂/Water/Mineral wettability becomes significant for trapping capacities. Thus,
80 this work aims to benchmark the influence of trace concentrations of such organics and the
81 effect of their carbon chain length on CO₂-rock wettability.

82

83

84 **2. Experimental Methodology**

85 **2.1. Materials**

86 Nine pure quartz samples (Quartz (single crystals; testing chips from WARD'S Natural
87 Science; sample range = 12 mm to 19 mm x 10 mm x 10 mm) were used as a model for
88 sandstone storage formations. The surface roughnesses of all nine surfaces were provided by
89 the supplier and the values ranged from 1 nm to 2 nm (root-mean-square (RMS) surface
90 roughness, which is very smooth (Sarmadivaleh et al. 2015).


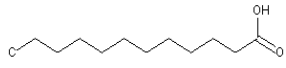
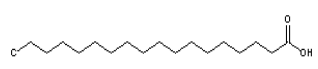
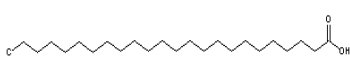
91 CO₂ (purity \geq 99.999 mol%; from BOC, gas code-082), N₂ (purity \geq 99.999 mol%; from BOC,
92 gas code-234) and 10 wt% NaCl brine (NaCl purity \geq 99.9mol%; from Scharlab) were used.

93 The NaCl was dissolved in deionized water (Ultrapure from David Gray; electrical
94 conductivity = 0.02 mS/cm). Subsequently, the NaCl brine was equilibrated with CO₂ at
95 experimental conditions in a high pressure mixing reactor (according to the procedure
96 described by El-Maghraby et al. 2012). To represent organic compounds, organic acids were
97 selected due to their presence in hydrocarbon reservoirs and aquifers; these included hexanoic
98 acid, lauric acid, stearic acid, and lignoceric or oleic acid (Jardine et al., 1989; Legens et al.,
99 1998; Madsen and Ida, 1998; Hansen et al., 2000; Amaya et al., 2002; Hamouda and Gomari,

100 2006; Kharaka et al., 2009; Stalker et al., 2013; Yang et al., 2015), Tabe 1 (purchased from
101 Sigma Aldrich, purity \geq 98 mol%).

102

103 Table 1: Properties of organic acids used in this study.

Organic Acid	Physical state	Formula	Number of C atoms	Molar mass (g/mol)	Chemical Structure
Hexanoic acid	Liquid	C ₆ H ₁₂ O ₂	6	116.158	
Lauric acid	solid	C ₁₂ H ₂₄ O ₂	12	200.318	
Stearic acid	solid	C ₁₈ H ₃₆ O ₂	18	284.4772	
Lignoceric acid	solid	C ₂₄ H ₄₈ O ₂	24	368.63	

104

105

106 Acetone (\geq 99.9 mol%; from Rowe Scientific) was used as surface cleaning agent, and drops
107 of aqueous hydrochloric acid (ACS reagent, concentration 37 vol%, Sigma Aldrich) were used
108 to control the pH of the brine (see ageing procedure below for more details).

109

110 2.2. Sample preparation

111 2.2.1 Quartz surface preparation

112 Initially the mineral (quartz) substrates were cleaned with DI-water to remove any dust or
113 surface fragments from the surface. The sample was then dried in an oven at 90°C for 60 mins
114 and exposed to air plasma (using a DiemerYocto instrument) for 15 mins to remove any organic
115 contamination (Love et al., 2005; Iglauer et al., 2014).

116 2.2.2 Ageing procedure

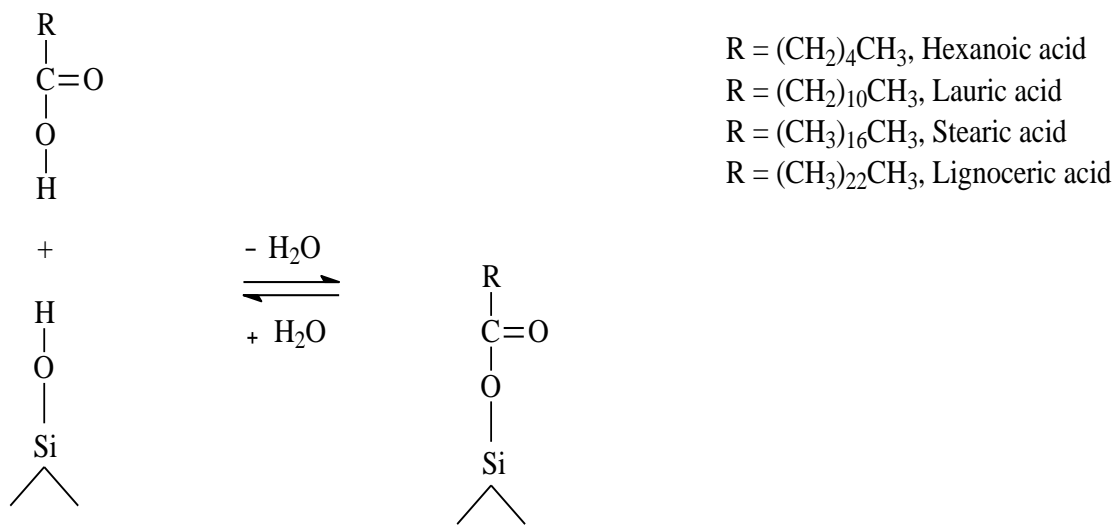
117 To mimic a typical storage formation, where the rock pore surfaces were exposed to formation
118 water over geological times we adopted the following strategy (Davis 1982; Ulrich et al., 1988;
119 Zullig and Morse, 1988; Ochs et al., 1994; Hoeiland et al., 2001; White et al., 2003; Nordbotten
120 et al., 2005; Karoussi et al., 2008; Birkholzer et al., 2009; Ji et al., 2015; Kleber et al., 2015):

121 The quartz samples were immersed for 30 mins in 2 wt% NaCl brine at ambient conditions,
122 while the acidity was maintained at pH = 4 by adding drops of aqueous hydrochloric acid; this
123 procedure increases the adsorption rate of organics onto the substrate, and thus simulates
124 adsorption of organic molecules over geological times (i.e. millions of years' exposure time)
125 (Thurman 1985; Jardine et al., 1989; Madsen and Ida, 1998; Kharaka et al., 2009; Stalker et al.
126 2013; Yang et al., 2015). Ultraclean N₂ was then used to mechanically clean (blow away) the
127 remaining water from the surface to avoid contamination. Subsequently the substrates were
128 aged in different organic acid/n-decane solutions of prescribed molarity (10⁻² M to 10⁻¹⁰ M
129 organic acid concentration) for seven days to mimic exposure to formation fluid (which
130 contains organic molecules) over geological time (Thurman 1985; Jardine et al., 1989; Madsen
131 and Ida, 1998; Kharaka et al., 2009; Stalker et al. 2013; Yang et al., 2015).

132 Previously, silanes were used to render the wettability of quartz surfaces oil-wet. Typically,
133 different silanes have different impacts on surfaces hydrophilicity (Dickson et al., 2006, Grate
134 et al., 2012, Hobeika et al., 2017). However, organic acids including stearic acids represent
135 more realistically subsurface environments (Al-Anssari et al., 2016, 2018, Paterson et al., 2011,
136 Hamouda et al., 2006, Gomari et al., 2006); while silanes do not exist in the subsurface (due to
137 their high reactivity).

138 It is vital to re-create such mineral surfaces to realistically mimic the subsurface behaviour,
139 particularly with respect to their wettability characteristics (Davis 1982; Ochs et al., 1994;

140 Adamson and Gast 1997; Kleber et al., 2015). Note that it is proven that carboxylic acids and
 141 hydrocarbons both exist in deep saline aquifers (Bennett et al., 1993), as a result of
 142 biodegradation and organic matter diagenesis and subsequent migration into the water zones
 143 (Jones et al., 2008).
 144 Mechanistically, the organic acid esterifies the hydroxyl groups on the quartz surface in a
 145 condensation reaction (Scheme 1).



146

147 **Scheme 1.** Chemisorption of organic acids on solid quartz surface (\wedge indicates solid bulk).

148 Thus carboxylic components are chemically (covalently) bonded to the quartz surface,
 149 rendering them strongly hydrophobic (Al-Anssari et al., 2016).

150

151 **2.3. Surface characterization of pure and aged quartz surfaces**

152 The surface properties of the quartz samples were analysed via energy dispersive X-ray
 153 spectroscopy (EDS, Oxford X-act SSD X-ray detector with Inca and Aztec software) and
 154 contact angle (θ) measurements. Table 2 lists the EDS results before and after aging; these are
 155 average elemental surface concentrations (these are average over 45 data points: 5 data points

156 measured on each sample, on nine different samples) for each acid tested. Surface coverages
 157 with organic acid are also given (determined via the method defined by Dickson et al. 2006).
 158 Table 2. Surface composition of pure and aged quartz samples and associated surface coverage
 159 with all organic acids.

Concentration ion (Molarity)	Pure Quartz			After ageing			Change due to ageing			Estimated surface coverage (after Dickson et al., 2006) $\left(1 - \frac{wt\% C_{before\ aging}}{wt\% C_{after\ aging}}\right) \times 100$
	wt% Si	wt% C	wt% O	wt% Si	wt% C	wt% O	wt% Si	wt% C	wt% O	
Hexanoic Acid										
10 ⁻²	31.9	2.3	65.8	38.1	4.8	57.1	+6.2	+2.5	-8.7	52.1
10 ⁻³	33.3	4.1	62.6	30.3	7.5	62.2	-3.0	+3.4	-0.4	45.3
10 ⁻⁴	35.4	2.8	61.8	37.0	4.9	58.1	+1.6	+2.1	-3.7	42.9
10 ⁻⁵	34.7	3.2	62.1	34.2	5.1	60.7	-0.5	+1.9	-1.4	37.3
10 ⁻⁶	29.0	3.5	67.5	32.9	5.2	61.9	+3.9	+1.7	-5.6	32.7
10 ⁻⁷	29.5	4.2	66.3	29.0	5.8	65.2	-0.5	+1.6	-1.1	27.6
10 ⁻⁸	32.8	1.8	65.4	48.0	2.3	49.7	+15.2	+0.5	-15.7	21.7
10 ⁻⁹	29.9	3.4	66.7	33.1	4.1	62.8	+3.2	+0.7	-3.9	17.1
10 ⁻¹⁰	31.8	2.6	65.6	32.0	2.9	65.1	+0.2	+0.3	-0.5	10.3
0	34.0	1.5	64.5	34.0	1.5	64.5	0	0	0	0
Lauric Acid										
10 ⁻²	38.1	2.4	59.5	27.6	5.3	67.1	-10.5	+2.9	+7.6	54.7
10 ⁻³	33.8	1.8	64.4	31.1	3.5	65.4	-2.7	+1.7	+1.0	48.6
10 ⁻⁴	33.0	3.4	63.6	28.8	6.1	65.1	-4.2	+2.7	+1.5	44.3
10 ⁻⁵	38.3	4.3	57.4	35.4	7.1	57.5	-2.9	+2.8	+0.1	39.4
10 ⁻⁶	32.4	2.6	65.0	34.1	4.0	61.9	+1.7	+1.4	-3.1	35.0
10 ⁻⁷	34.5	3.6	61.9	33.5	5.2	61.3	-1.0	+1.6	-0.6	30.8
10 ⁻⁸	32.4	4.1	63.5	32.7	5.4	61.9	+0.3	+1.3	-1.6	24.1
10 ⁻⁹	32.4	1.4	66.2	36.1	1.7	62.2	+3.7	+0.3	-4.0	17.6
10 ⁻¹⁰	32.2	3.5	64.3	32.8	4.1	63.1	+0.6	+0.6	-1.2	14.6
0	31.6	2.3	66.1	31.6	2.3	66.1	0	0	0	0
Stearic Acid										
10 ⁻²	35.4	1.3	63.3	32.2	3.1	64.7	-3.2	+1.8	+1.4	58.1
10 ⁻³	34.3	3.7	62.0	26.8	7.6	65.6	-7.5	+3.9	+3.6	51.3
10 ⁻⁴	37.0	4.5	58.5	26.7	8.4	64.9	-10.3	+3.9	+6.4	46.4
10 ⁻⁵	36.8	1.6	61.6	32.3	2.8	64.9	-4.5	+1.2	+3.3	42.9
10 ⁻⁶	35.8	2.4	61.8	41.7	3.8	54.5	+5.9	+1.4	-7.3	36.8
10 ⁻⁷	36.0	4.3	59.7	22.0	6.3	71.7	-14.0	+2.0	+12	31.7
10 ⁻⁸	38.2	2.9	58.9	23.8	4.0	72.2	-14.4	+1.1	+13.3	27.5
10 ⁻⁹	34.1	4.2	61.7	23.5	5.2	71.3	-10.6	+1.0	+9.6	19.2
10 ⁻¹⁰	36.5	4.1	59.4	45.4	4.9	49.7	+8.9	+0.8	-9.7	16.3
0	36.5	2.2	61.3	36.5	2.2	61.3	0	0	0	0
Lignoceric Acid										
10 ⁻²	37.3	2.3	60.4	25.0	6.2	68.8	-12.3	+3.9	+8.4	62.9
10 ⁻³	36.3	2.0	61.7	25.4	4.6	70.0	-10.9	+2.6	+8.3	56.5
10 ⁻⁴	34.1	4.0	61.9	21.9	7.8	70.3	-12.2	+3.8	+8.4	48.7
10 ⁻⁵	35.6	3.4	61.0	24.8	6.2	69.0	-10.8	+2.8	+8.0	45.2
10 ⁻⁶	34.7	3.5	61.8	32.3	5.8	61.9	-2.4	+2.3	+0.1	39.7
10 ⁻⁷	33.9	4.1	62.0	28.9	6.1	65.0	-5.0	+2.0	+3.0	32.8
10 ⁻⁸	33.7	2.7	63.6	26.0	3.9	70.1	-7.7	+1.2	+6.5	30.8
10 ⁻⁹	39.6	1.9	58.5	27.7	2.5	69.8	-11.9	+0.6	+11.3	24.0
10 ⁻¹⁰	36.5	4.2	59.3	25.0	5.1	69.9	-11.5	+0.9	+10.6	17.6

0	34.0	3.6	62.4	34.0	3.6	62.4	0	0	0	0
---	------	-----	------	------	-----	------	---	---	---	---

160

161

162 Table 3. Average Elemental surface analysis of quartz samples before and after ageing.

Organic Acids	Before aging			After aging		
	Si (wt%)	C (wt%)	O (wt%)	Si (wt%)	C (wt%)	O (wt%)
Hexanoic acid	32.2 ^a ± 3.2 ^b	2.9 ^a ± 1.4 ^b	64.8 ^a ± 2.9 ^b	34.9 ^a ± 9.5 ^b	4.4 ^a ± 3.0 ^b	60.7 ^a ± 7.8 ^b
Lauric acid	33.9 ^a ± 3.4 ^b	2.9 ^a ± 1.5 ^b	63.2 ^a ± 4.4 ^b	32.4 ^a ± 4.3 ^b	4.5 ^a ± 2.7 ^b	63.2 ^a ± 4.8 ^b
Stearic acid	36.1 ^a ± 2.1 ^b	3.1 ^a ± 1.6 ^b	60.8 ^a ± 2.4 ^b	31.1 ^a ± 11.7 ^b	4.8 ^a ± 3.1 ^b	64.1 ^a ± 11.3 ^b
Lignoceric acid	35.6 ^a ± 3.0 ^b	3.2 ^a ± 1.2 ^b	61.3 ^a ± 2.6 ^b	27.1 ^a ± 6.1 ^b	5.2 ^a ± 2.7 ^b	67.7 ^a ± 4.2 ^b

163

164 ^a average surface concentration is based on the arithmetic average of 45 data points measured on five
165 different sites for each of the nine samples at all concentrations tested.

166 ^b '±' values are the standard deviations of these observations.

167

168 Clearly, aging had a significant impact on the atomic surface concentrations irrespective of the

169 type and concentration of organic acid (Table 3). A significant overall average increase in

170 surface carbon concentration (+1.6 wt% C for Hexanoic Acid, +1.7 wt% C for Lauric Acid,

171 +1.9 wt% C for Stearic Acid and +2.2 wt% C for Lignoceric Acid) was measured. These

172 changes in atomic coverage were caused by the chemisorption of the carboxylic acid on the

173 quartz surface, consistent with Zullig and Morse (1988); see also 2.2.2 and scheme 1 above.

174 Moreover, the brine contact angles on the pure quartz samples were 0° (advancing and

175 receding) at ambient conditions, thus pure quartz was completely water-wet at ambient

176 conditions. However, higher contact angles (advancing 56° and receding 54° ± 3°) were

177 measured at reservoirs conditions on these pure quartz samples (323 K (50 °C), 25 MPa),

178 consistent with literature data (Chiquet et al., 2007; Farokhpoor et al., 2013; Al-Yaseri et al.

179 2016a,b; Arif et al., 2016d;). However, aging of the quartz surfaces caused a significant change
180 in contact angles and thus CO₂-wettability, this is discussed in detail below.

181

182 **2.4. Contact angle measurements**

183 Contact angle measurements are a standard technique for assessing the wettability behaviour
184 of a given rock/fluid/fluid system. Here we used the tilted plate technique, which is regarded
185 as the most effective contact angle measurement method as it can measure advancing and
186 receding contact angles simultaneously (Lander et al., 1993).

187 The schematic of the experimental setup is shown in Figure 1. It consists of a high pressure-
188 high temperature cell, which houses the sample inside on a tilted plate. The cell is connected
189 to two pumps (Teledyne D-500, pressure accuracy of 0.1%) used for either discharging brine
190 or CO₂. Furthermore, a CO₂ gas cylinder and the brine pump are both connected to a mixing
191 reactor with which CO₂ and brine can be thermodynamically equilibrated (El-Maghraby et al.
192 2012).

193 Initially, the cell was charged with CO₂ at the desired measurement pressure and temperature
194 (0.1 MPa, 25 MPa and 323 K (50 °C)). Temperature of the pumps was controlled through
195 heating bath and the cell temperature was controlled through heating tape around it. The brine
196 pump was initially filled with CO₂-equilibrated brine (equilibrated at experimental conditions)
197 and a droplet of equilibrated brine (average drop volume was 6 μL (± 1 μL) was dispensed
198 onto the quartz surface through a needle. The advancing (θ_a) and receding (θ_r) brine contact
199 angles were then measured at the leading and trailing edge of the droplet just before the drop
200 started to move (Lander et al., 1993). This process was recorded by a high performance video
201 camera (Basler scA 640–70 fm, pixel size = 7.4 μm; frame rate = 71 fps; Fujinon CCTV lens:
202 HF35HA-1B; 1:1.6/35 mm), which was connected to a computer system to display and analyse

203 the results. The standard deviation of the measurements was $\pm 3^\circ$ based on replicated
204 measurements.

205

206

207

208

209

210

211

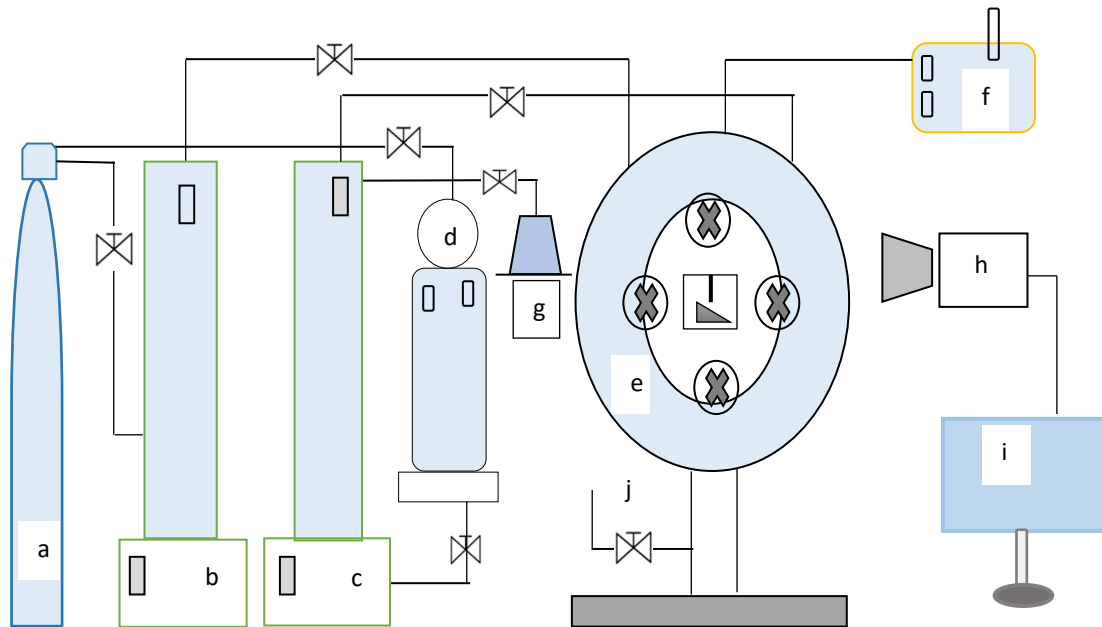
212

213

214

215

216



216

217 Figure 1. Experimental setting used in this study for measuring advancing and receding contact
218 angles (modified after Arif et al., 2017a). (a) CO₂ cylinder (b) high precision syringe pump-
219 CO₂, (c) high precision syringe pump-water, (d) High pressure Parr reactor for fluid
220 equilibration e) high pressure cell with substrate housed on a tilted plate inside, (f) heating unit,
221 (g) liquid feed/drain system, (h) high resolution video camera, (i) image visualization and
222 interpretation software, (j) pressure relief valve.

223

224 3. Results and Discussion

225 Our results show that the quartz surface loses its water-wetness with increasing organic acid
226 concentration. However, at organic acid concentrations $\leq 10^{-6}$ M, contact angles were only
227 minimally affected, Figure 6, and thus structural trapping is not significantly affected (note:

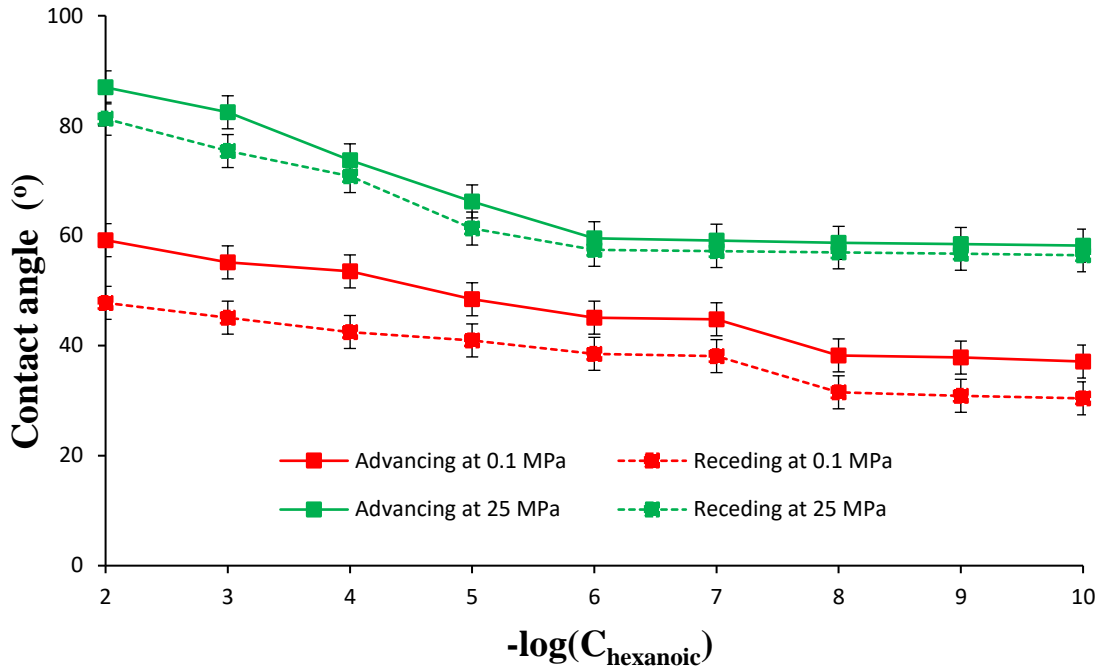
228 even at low concentrations $\leq 10^{-6}$ M optimal residual trapping capacities are significantly
229 affected). However, for concentrations $> 10^{-6}$ M, quartz wetting behaviour shifts from strongly
230 water-wet to an intermediate-wet state (Iglauer et al., 2015b). A recent study conducted on
231 carbonate minerals (Ali et al., 2019) showed that even at low organic concentrations ($\leq 10^{-6}$ M
232 organic acid), optimal residual trapping capacities could be affected, which is due to the surface
233 coverage of the mineral with organic acid and its tendency to alter the formation more CO₂-
234 wet. Such wettability alteration changes the primary drainage capillary pressure curve (Morrow
235 1970, Anderson 1986, Masalmeh 2003), and thus the initial CO₂ saturation directly influencing
236 the residual CO₂ saturation (e.g. Pentland et al. 2011; Wang et al., 2015, Heshmati et al., 2014,
237 Akbarabadi et al., 2015).

238

239 **3.1. Effect of acid concentration on quartz wettability**

240 Advancing and receding brine contact angles increased significantly with an increase in organic
241 acid concentration, as shown in Figures 2-5.

242



243

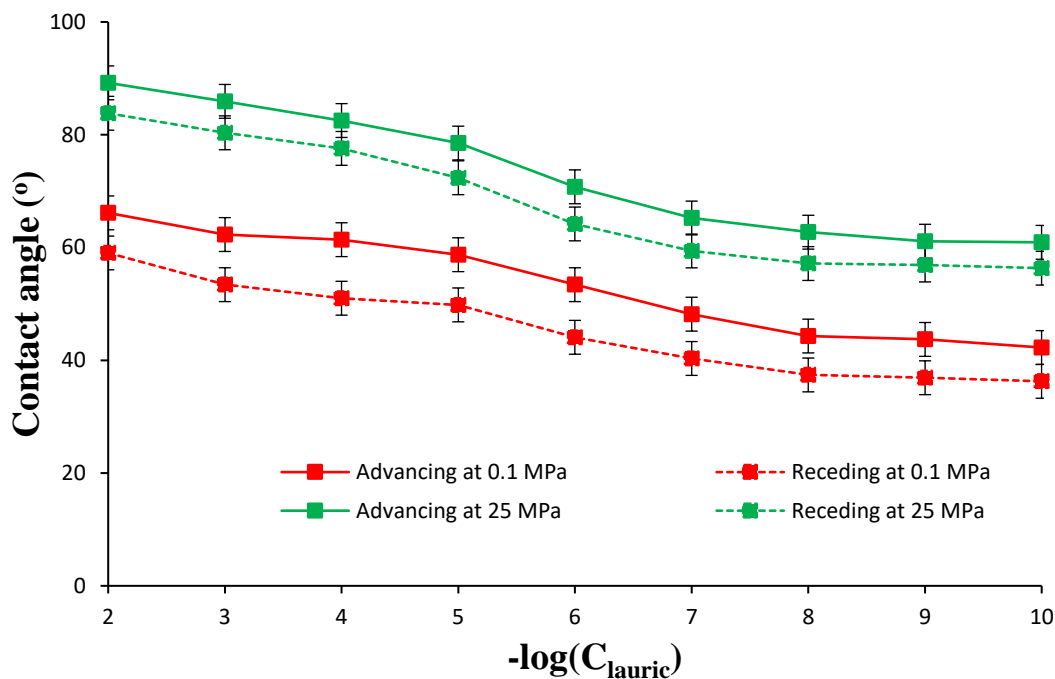
244 Figure 2. Quartz/CO₂/brine contact angles (measured through the water) as a function of
 245 hexanoic acid (C₆) concentration; C_{hexanoic} is the hexanoic acid concentration (molarity). Solid
 246 lines: advancing; dotted lines: receding. Red: ambient pressure; green: 25 MPa and 323 K (50
 247 °C).

248

249 The contact angle was significantly higher at high pressure, consistent with literature data (e.g.
 250 Dickson et al. 2006; Espinoza and Santamarina 2010; Broseta et al. 2012; Shojai Kaveh et al.,
 251 2012, 2016; Chen et al, 2015; Iglauer et al., 2015a,b; Al-Yaseri et al. 2016a,b; Iglauer 2017).
 252 For example, at 25 MPa and 323 K (50 °C), for the quartz surface aged in 10⁻¹⁰ M hexanoic
 253 acid, θ_a was 58° and θ_r was 55° implying that the quartz surface is weakly water-wet under such
 254 conditions. With an increase in hexanoic acid concentration up to 10⁻⁶ M, there was an
 255 insignificant change in θ. However, further organic acid concentration increase resulted in
 256 significant contact angle increase. For instance, when the hexanoic acid concentration
 257 increased to 10⁻² M, at the same temperature and pressure (25 MPa, and 323 K (50 °C)), θ_a and
 258 θ_r increased to 87° and 82°, implying a wettability transformation from weakly water-wet to

259 intermediate-wet. Such a reduction in water wettability of the surface potentially leads to a
 260 reduction in residual trapping capacities where CO₂ plume is migrating in storage formation
 261 (Chaudhary et al., 2013; Iglauer et al., 2017; Al-Menhali et al., 2016a; Rahman et al., 2016).
 262 Note for instance that lower residual CO₂ saturations have been measured in more hydrophobic
 263 rock by x-ray micro-tomography (Al-Menhali et al., 2016a, Chaudhary et al., 2013, Rahman et
 264 al., 2016).
 265 Lauric acid followed somewhat similar trends. For the quartz surface aged in 10⁻¹⁰ M lauric
 266 acid, quartz/CO₂/water contact angles were significantly lower than those measured on surfaces
 267 aged in 10⁻² M lauric acid. Thus higher organic concentrations render the surface more non-
 268 wetting to water. For example, at 25 MPa and 323 K (50 °C), for the quartz surface aged in 10⁻
 269 ¹⁰ M lauric acid, θ_a measured as 61° and θ_r as 56°, which increased to $\theta_a = 89^\circ$ and $\theta_r = 84^\circ$
 270 when lauric acid concentration increased to 10⁻² M (Figure 3).

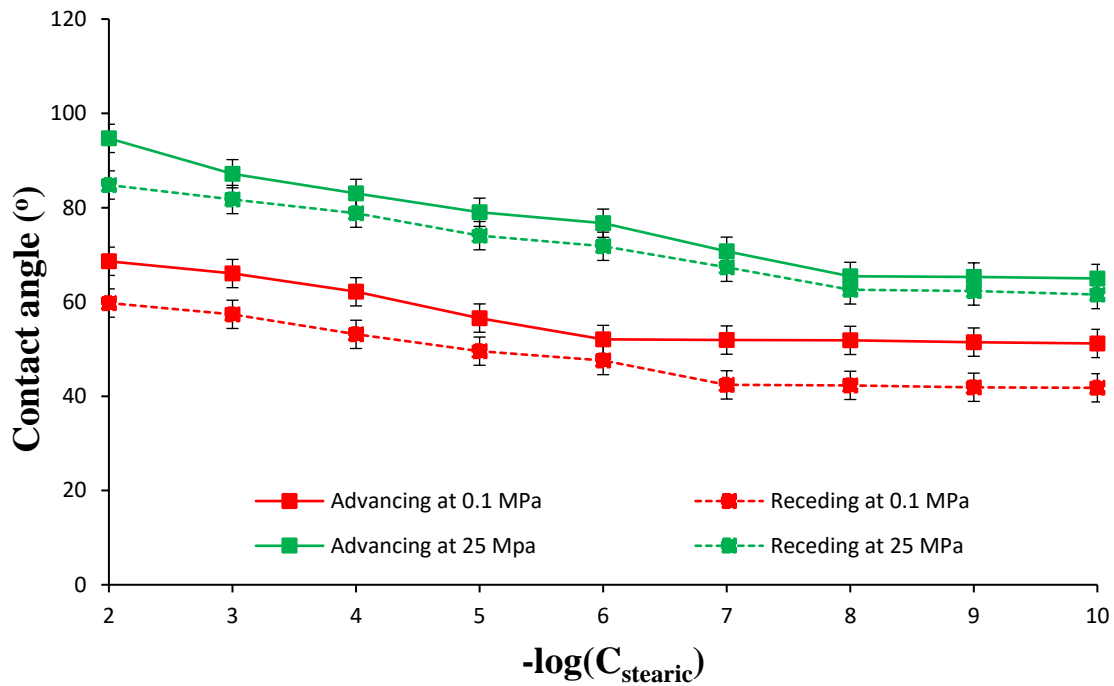
271



272

273 Figure 3. Quartz/CO₂/brine contact angles as a function of lauric acid (C₁₂) concentration; C_{lauric}
 274 is the lauric acid concentration (molarity). Solid lines: advancing; dotted lines: receding. Red:
 275 ambient pressure; green: 25 MPa and 323 K (50 °C).

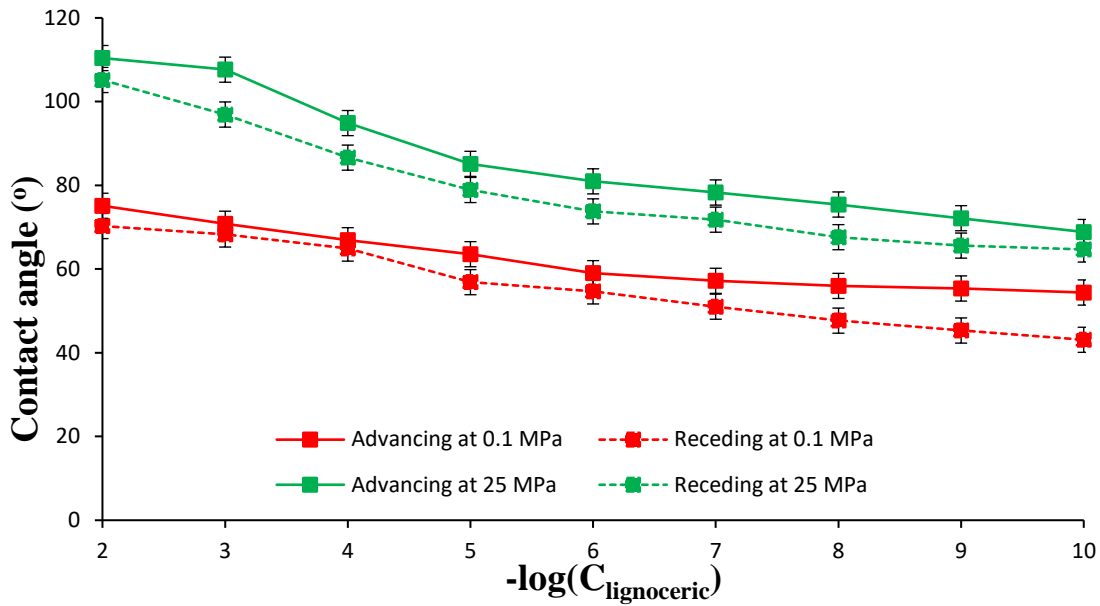
276



277

278 Figure 4. Quartz/CO₂/brine contact angles as a function of stearic acid (C₁₈) concentration;
 279 C_{stearic} is the stearic acid concentration (molarity). Solid lines: advancing; dotted lines: receding.
 280 Red: ambient pressure; green: 25 MPa and 323 K (50 °C).

281



282

283 Figure 5. Quartz/CO₂/brine contact angles as a function of lignoceric acid (C₂₄) concentration;
 284 C_{lignoceric} is the lignoceric acid concentration (molarity). Solid lines: advancing; dotted lines:
 285 receding. Red: ambient pressure; green: 25 MPa and 323 K (50 °C).

286

287 The results showed the same trend for quartz surfaces aged in stearic acid and lignoceric acid
 288 (Figures 4 and 5). In summary, the higher the organic acid concentration was, the higher were
 289 the values of both the advancing and receding water contact angles irrespective of the type of
 290 organic acid used for aging. Our results are consistent with literature data on wettability of
 291 calcite/oil/brine systems in the presence of organic acids (Hansen et al., 2000; Standness and
 292 Austad, 2003; Gomari et al., 2006). Mechanistically, carboxylic acid adsorbs onto the quartz
 293 surface leading to a wettability modification towards less water-wet surface conditions, see
 294 above.

295 When compared with CO₂-wettability of pure quartz surfaces, we find that higher contact
 296 angles are found, even at the lowest organic acid concentration (10⁻¹⁰ M, which is very low).
 297 For instance, for pure quartz/CO₂/brine system, at 20 MPa and 323 K (50 °C), θ_a was reported
 298 to be approximately 40° (Sarmadivaleh et al., 2015), whereas the lowest θ_a in the presence of

299 lowest chain organic acid (Hexanoic acid, C₆) was 57° (Figure 6). It is thus clear that even
300 minute amounts of organic acid significantly increase the CO₂-wettability of mineral surfaces.
301 As such minute concentrations always exist in the subsurface, even in aquifers (Bennett et al.,
302 1993; Jones et al., 2008; Stalker et al. 2013), lower residual trapping capacities than previously
303 thought are expected (Ali et al., 2019).

304

305 **3.2 Influence of organic acid alkyl chain length on quartz wettability**

306 It is clear that all organic acids influence the quartz wettability in a similar fashion i.e. both
307 water advancing and receding contact angles increase with an increase in organic acid
308 concentration and quartz rapidly loses its water-wetness, Figure 6. However, at a fixed organic
309 acid concentration, the absolute values of contact angles were different for different acids
310 (which differ in their alkyl chain length and their coverage on the quartz surface, as showed in
311 Figure 6); surfaces aged in hexanoic acid (C₆) exhibited the lowest contact angles values, while
312 surfaces aged in lignoceric acid (C₂₄) exhibited the highest contact angles values. Lauric acid
313 and stearic acid fell in between. For instance, at 25 MPa and 323 K (50 °C), and a fixed organic
314 concentration 10⁻² M of hexanoic, lauric , stearic and lignoceric acid, $\theta_r = 81^\circ$, $\theta_r = 84^\circ$, $\theta_r =$
315 85° and $\theta_r = 105^\circ$, respectively. Such a wettability transformation from intermediate-wet to
316 CO₂-wet is attributed to the number of carbon atoms present in the acid, Table 1. Clearly, longer
317 alkyl chains in the organic acid renders the surface more hydrophobic.

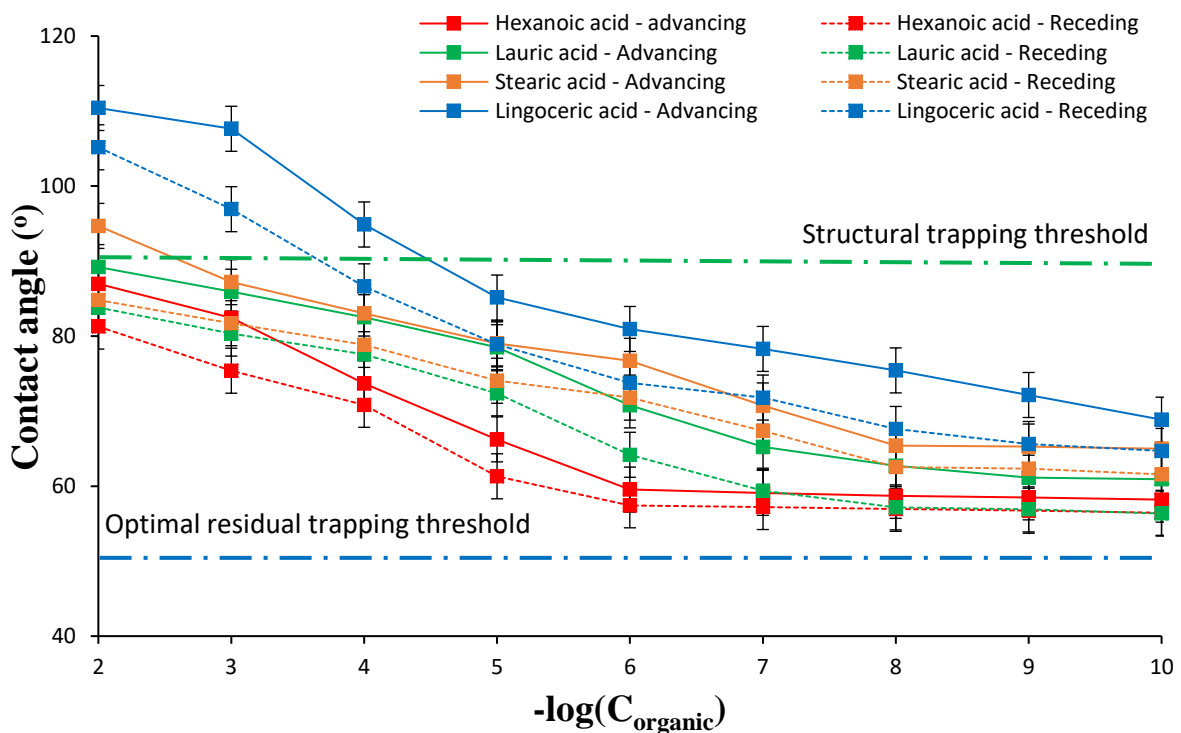
318 These effects have dramatic impact on the optimal residual trapping limit, which we consider
319 here as the point where primary drainage is unaffected by wettability, i.e. at $\theta_a = 50^\circ$ (Morrow
320 1970, Morrow 1976). For example, at 25 MPa and 323 K (50 °C) and a fixed trace organic
321 concentration of 10⁻¹⁰ M, $\theta_a > 50^\circ$ for all acids (note that this is a very minute concentration,
322 and much higher organic concentrations were measured in deep saline aquifers (e.g. Thurman

323 1985; Jardine et al., 1989; Madsen and Ida, 1998; Kharaka et al., 2009; Stalker et al. 2013;
 324 Yang et al., 2015)); Figure 6.

325 Overall it is clear that a detailed knowledge of organic acids and its relative concentrations in
 326 storage formations is very important for assessing the feasibility of long-term geological
 327 storage projects.

328

329



330

331

332 Figure 6. Quartz/CO₂/brine contact angles as a function of organic acid concentration and alkyl
 333 chain length at 25 MPa and 323 K (50 °C); C_{organic} is the organic acid concentration (molarity).

334 Dotted blue horizontal lines in the graph define the capillary trapping threshold ($\theta = 50^\circ$), and
 335 dotted green horizontal lines in graph define the structural trapping ($\theta > 90^\circ$) threshold.

336

337

338

339 4. Conclusions

340 Deep saline aquifers contain organic acids, which have a direct impact on the interfacial
341 phenomena at the fluid/rock interface due to chemisorption. These effects are, however, only
342 poorly understood; thus we measured the wettability of quartz/CO₂/brine systems in the
343 presence of various organic acids. Four acids (hexanoic acid, lauric acid, stearic acid, lignoceric
344 acid) were considered for a wide range of concentrations (10⁻⁹ M to 10⁻² M), and advancing
345 and receding contact angles were measured at typical storage conditions (25 MPa and 323 K
346 (50 °C), as well as at ambient pressure) in order to mimic a realistic subsurface behaviour. We
347 found that both advancing and receding contact angles increased with an increase in organic
348 acid concentration throughout the tested experimental matrix. In addition, at a fixed organic
349 acid concentration, the highest contact angles values were measured for lignoceric acid (C24),
350 while relatively least values were recorded for hexanoic acid (C6). This behaviour is attributed
351 to the number of carbon atoms in the organic acids alkyl chain, and hence a higher number of
352 C atoms, resulting in more CO₂-wet/hydrophobic surfaces, which causes a reduction in residual
353 trapping capacities.

354 We thus conclude that CO₂ geological storage capacities in certain geological scenarios
355 (aquifers as an example) may be lower than previously thought. Reservoir-scale models thus
356 need to take these effects into account so that accurate storage predictions are obtained thus de-
357 risking carbon geological storage (CGS) projects.

358

359

360

361

362

363

364 **Conflicts of Interest**

365 There are no conflicts to declare.

366

367

368 **Acknowledgments**

369 The first author acknowledges the support provided from Australian Government and Curtin

370 University for providing Research Training Program Scholarship for his research studies. The

371 authors declare no competing financial interests.

372

373

374

375

376

377

378

379

380

381

382

383

384

385

386

387

388

389

390 References

- 391 A. W. Adamson, & A. P. Gast, *Physical Chemistry of Surfaces*, 6th ed., Wiley-Interscience, N. Y., 1997.
392
- 393 Agartan, E., Trevisan, L., Cihan, A., Birkholzer, J., Zhou, Q., & Illangasekare, T. H. (2015). Experimental study
394 on effects of geologic heterogeneity in enhancing dissolution trapping of supercritical CO₂. *Water Resources*
395 *Research*, 51(3), 1635-1648, doi: 10.1002/2014WR015778
396
- 397 Akbarabadi, M., & Piri, M. (2015). Co-sequestration of SO₂ with supercritical CO₂ in carbonates: An experimental
398 study of capillary trapping, relative permeability, and capillary pressure. *Advances in water resources*, 77, 44-5,
399 doi: 10.1016/j.advwatres.2014.08.011
- 400 Al-Anssari, S., Barifcani, A., Wang, S., Lebedev, M., & Iglauer, S. (2016). Wettability alteration of oil-wet
401 carbonate by silica nanofluid. *Journal of Colloid and Interface Science*, 461, 435-442.
402 doi:http://dx.doi.org/10.1016/j.jcis.2015.09.051
- 403 Al-Anssari, S., Arif, M., Wang, S., Barifcani, A., Lebedev, M., & Iglauer, S. (2018). Wettability of nanofluid-
404 modified oil-wet calcite at reservoir conditions. *Fuel*, 211, 405-414.
405 doi:https://doi.org/10.1016/j.fuel.2017.08.111
- 406 Al-Khdheawi, E. A., Vialle, S., Barifcani, A., Sarmadivaleh, M., & Iglauer, S. (2016). Influence of CO₂-
407 wettability on CO₂ migration and trapping capacity in deep saline aquifers. *Greenhouse Gases: Science and*
408 *Technology*, 7(2), 328-338, doi: 10.1002/ghg.1648
409
- 410 Al-Khdheawi, E. A., Vialle, S., Barifcani, A., Sarmadivaleh, M., & Iglauer, S. (2017). Impact of reservoir
411 wettability and heterogeneity on CO₂-plume migration and trapping capacity. *International Journal of Greenhouse*
412 *Gas Control*, 58, 142-158, doi: 10.1016/j.ijggc.2017.01.012
413
- 414 Al-Menhali, A. S., Menke, H. P., Blunt, M. J., & Krevor, S. C. (2016a). Pore Scale Observations of Trapped CO₂
415 in Mixed-Wet Carbonate Rock: Applications to Storage in Oil Fields. *Environmental Science &*
416 *Technology*, 50(18), 10282-10290, doi: 10.1021/acs.est.6b03111
417
- 418 Al-Menhali, A. S., & Krevor, S. (2016b). Capillary trapping of CO₂ in oil reservoirs: Observations in a mixed-
419 wet carbonate rock. *Environmental science & technology*, 50(5), 2727-2734, doi: 10.1021/acs.est.5b05925
420
- 421 Al-Yaseri, A. Z., Lebedev, M., Barifcani, A., & Iglauer, S. (2016)a. Receding and advancing (CO₂+ brine+ quartz)
422 contact angles as a function of pressure, temperature, surface roughness, salt type and salinity. *The Journal of*
423 *Chemical Thermodynamics*, 93, 416-423, doi: 10.1016/j.jct.2015.07.031
424
- 425 Al-Yaseri, A. Z., Roshan, H., Lebedev, M., Barifcani, A., & Iglauer, S. (2016)b. Dependence of quartz wettability
426 on fluid density. *Geophysical Research Letters*, 43(8), 3771-3776, doi: 10.1002/2016GL068278
427
- 428 Ali, M., Al-Anssari, S., Arif, M., Barifcani, A., Sarmadivaleh, M., Stalker, L., . . . Iglauer, S. (2019). Organic acid
429 concentration thresholds for ageing of carbonate minerals: Implications for CO₂ trapping/storage. *Journal of*
430 *Colloid and Interface Science*, 534, 88-94. doi:https://doi.org/10.1016/j.jcis.2018.08.106
431
- 432 Amaya, J., Rana, D., & Hornof, V. (2002). Dynamic interfacial tension behavior of water/oil systems containing
433 in situ-formed surfactants. *Journal of Solution Chemistry*, 31(2), 139-148, doi: 10.1023/A:1015201119955
434
- 435 Anderson, W. G. (1986). Wettability Literature Survey. 3. The Effects of Wettability on the Electrical-Properties
436 of Porous-Media. *Journal of Petroleum Technology*, 38(13), 1371-1378, doi: 10.2118/13934-PA
437
- 438 Arif, M., Al-Yaseri, A. Z., Barifcani, A., Lebedev, M., & Iglauer, S. (2016)a. Impact of pressure and temperature
439 on CO₂-brine-mica contact angles and CO₂-brine interfacial tension: Implications for carbon geo-
440 sequestration. *Journal of colloid and interface science*, 462, 208-215, doi: 10.1016/j.jcis.2015.09.076
441
- 442 Arif, M., Barifcani, A., Lebedev, M., & Iglauer, S. (2016)b. Structural trapping capacity of oil-wet caprock as a
443 function of pressure, temperature and salinity. *International Journal of Greenhouse Gas Control*, 50, 112-120, doi:
444 10.1016/j.ijggc.2016.04.024
445

446 Arif, M., Barifcani, A., & Iglauer, S. (2016)c. Solid/CO₂ and solid/water interfacial tensions as a function of
447 pressure, temperature, salinity and mineral type: Implications for CO₂-wettability and CO₂ geo-
448 storage. *International Journal of Greenhouse Gas Control*, 53, 263-273, doi: 10.1016/j.ijggc.2016.08.020
449

450 Arif, M., Barifcani, A., & Iglauer, S. (2016)d. Solid/CO₂ and solid/water interfacial tensions as a function of
451 pressure, temperature, salinity and mineral type: Implications for CO₂-wettability and CO₂ geo-storage.
452 *International Journal of Greenhouse Gas Control*, 53, 263-273, doi: 10.1016/j.ijggc.2016.08.020
453

454 Arif, M., Lebedev, M., Barifcani, A., & Iglauer, S. (2017)a. CO₂ storage in carbonates: Wettability of
455 calcite. *International Journal of Greenhouse Gas Control*, 62, 113-121, doi: 10.1016/j.ijggc.2017.04.014
456

457 Arif, M., Lebedev, M., Barifcani, A., & Iglauer, S. (2017)b. Influence of shale-total organic content on CO₂ geo-
458 storage potential. *Geophysical Research Letters*, doi: 10.1002/2017GL073532
459

460 Bennett, P. C., Siegel, D. E., Baedeker, M. J., & Hult, M. F. (1993). Crude oil in a shallow sand and gravel
461 aquifer—I. Hydrogeology and inorganic geochemistry. *Applied Geochemistry*, 8(6), 529-549, doi: 10.1016/0883-
462 2927(93)90012-6
463

464 Bikkina, P. K. (2011). Contact angle measurements of CO₂-water-quartz/calcite systems in the perspective of
465 carbon sequestration. *International Journal of Greenhouse Gas Control*, 5(5), 1259-1271, doi:
466 10.1016/j.ijggc.2011.07.001
467

468 Birkholzer, J. T., Zhou, Q., & Tsang, C. F. (2009). Large-scale impact of CO₂ storage in deep saline aquifers: a
469 sensitivity study on pressure response in stratified systems. *International Journal of Greenhouse Gas Control*, 3(2),
470 181-194, doi: 10.1016/j.ijggc.2008.08.002
471

472 Blunt, M., Fayers, F. J., & Orr Jr, F. M. (1993). Carbon dioxide in enhanced oil recovery. *Energy Conversion and*
473 *Management*, 34(9-11), 1197-1204, doi: 10.1016/0196-8904(93)90069-M
474

475 Broseta, D., Tonnet, N., & Shah, V. (2012). Are rocks still water-wet in the presence of dense CO₂ or
476 H₂S?. *Geofluids*, 12(4), 280-294, doi: 10.1111/j.1468-8123.2012.00369.x
477

478 Busch, A., Alles, S., Gensterblum, Y., Prinz, D., Dewhurst, D. N., Raven, M. D., ... & Krooss, B. M. (2008).
479 Carbon dioxide storage potential of shales. *International Journal of Greenhouse Gas Control*, 2(3), 297-308, doi:
480 10.1016/j.ijggc.2008.03.003
481

482 Chaudhary, K., Bayani Cardenas, M., Wolfe, W. W., Maisano, J. A., Ketcham, R. A., & Bennett, P. C. (2013).
483 Pore-scale trapping of supercritical CO₂ and the role of grain wettability and shape. *Geophysical Research*
484 *Letters*, 40(15), 3878-3882, doi: 10.1002/grl.50658
485

486 Chen, C., Wan, J., Li, W., & Song, Y. (2015). Water contact angles on quartz surfaces under supercritical CO₂
487 sequestration conditions: Experimental and molecular dynamics simulation studies. *International Journal of*
488 *Greenhouse Gas Control*, 42, 655-665, doi: 10.1016/j.ijggc.2015.09.019
489

490 Chiquet, P., Broseta, D., & Thibeau, S. (2007). Wettability alteration of caprock minerals by carbon
491 dioxide. *Geofluids*, 7(2), 112-122, doi: 10.1111/j.1468-8123.2007.00168.x
492

493 Davis, J. A. (1982). Adsorption of natural dissolved organic matter at the oxide/water interface. *Geochimica et*
494 *Cosmochimica Acta*, 46(11), 2381-2393, doi: 10.1016/0016-7037(82)90209-5
495

496 Dickson, J. L., Gupta, G., Horozov, T. S., Binks, B. P., & Johnston, K. P. (2006). Wetting phenomena at the
497 CO₂/water/glass interface. *Langmuir*, 22(5), 2161-2170, doi: 10.1021/la0527238
498

499 El-Maghraby, R. M., Pentland, C. H., Iglauer, S., & Blunt, M. J. (2012). A fast method to equilibrate carbon
500 dioxide with brine at high pressure and elevated temperature including solubility measurements. *The Journal of*
501 *Supercritical Fluids*, 62, 55-59, doi: 10.1016/j.supflu.2011.11.002
502

503 Espinoza, D. N., & Santamarina, J. C. (2010). Water-CO₂-mineral systems: Interfacial tension, contact angle, and
504 diffusion—Implications to CO₂ geological storage. *Water resources research*, 46(7), doi:
505 10.1029/2009WR008634

506
507 Farokhpoor, R., Bjørkvik, B. J., Lindeberg, E., & Torsæter, O. (2013). Wettability behaviour of CO₂ at storage
508 conditions. *International Journal of Greenhouse Gas Control*, 12, 18-25, doi: 10.1016/j.ijggc.2012.11.003
509
510 Gaines, G. L. (1966). Insoluble monolayers at liquid-gas interfaces.
511
512 Gaus, I. (2010). Role and impact of CO₂-rock interactions during CO₂ storage in sedimentary rocks. *International*
513 *journal of greenhouse gas control*, 4(1), 73-89, doi: 10.1016/j.ijggc.2009.09.015
514
515 Golding, S. D., Uysal, I. T., Boreham, C. J., Kirste, D., Baublys, K. A., & Esterle, J. S. (2011). Adsorption and
516 mineral trapping dominate CO₂ storage in coal systems. *Energy Procedia*, 4, 3131-3138, doi:
517 10.1016/j.egypro.2011.02.227
518
519 Gomari, K. R., & Hamouda, A. A. (2006). Effect of fatty acids, water composition and pH on the wettability
520 alteration of calcite surface. *Journal of petroleum science and engineering*, 50(2), 140-150, doi:
521 10.1016/j.petrol.2005.10.007
522
523 Grate, J. W., Dehoff, K. J., Warner, M. G., Pittman, J. W., Wietsma, T. W., Zhang, C., & Oostrom, M. (2012).
524 Correlation of Oil-Water and Air-Water Contact Angles of Diverse Silanized Surfaces and Relationship to Fluid
525 Interfacial Tensions. *Langmuir*, 28(18), 7182-7188. doi:10.1021/la204322k
526
527 Hamouda, A. A., & Rezaei Gomari, K. A. (2006, January). Influence of temperature on wettability alteration of
528 carbonate reservoirs. In *SPE/DOE Symposium on Improved Oil Recovery*. Society of Petroleum Engineers, doi:
529 10.2118/99848-MS
530
531 Hansen, G., Hamouda, A. A., & Denoyel, R. (2000). The effect of pressure on contact angles and wettability in
532 the mica/water/n-decane system and the calcite+ stearic acid/water/n-decane system. *Colloids and Surfaces A:*
533 *Physicochemical and Engineering Aspects*, 172(1), 7-16, doi: 10.1016/S0927-7757(99)00498-7
534
535 Heshmati, M., & Piri, M. (2014). Experimental investigation of dynamic contact angle and capillary rise in tubes
536 with circular and noncircular cross sections. *Langmuir*, 30(47), 14151-14162, doi: 10.1021/la501724y
537
538 Hobeika, N., Bouriat, P., Touil, A., Broseta, D., Brown, R., & Dubessy, J. (2017). Help from a Hindrance: Using
539 Astigmatism in Round Capillaries To Study Contact Angles and Wetting Layers. *Langmuir*, 33(21), 5179-5187.
540 doi:10.1021/acs.langmuir.7b01025
541
542 Hoeiland, S., Barth, T., Blokhus, A. M., & Skauge, A. (2001). The effect of crude oil acid fractions on wettability
543 as studied by interfacial tension and contact angles. *Journal of Petroleum Science and Engineering*, 30(2), 91-103,
544 doi: 10.1016/S0920-4105(01)00106-1
545
546 Iglauer, S. (2017). CO₂-Water-Rock Wettability: Variability, Influencing Factors, and Implications for CO₂
547 Geostorage. *Accounts of Chemical Research*, doi: 10.1021/acs.accounts.6b00602
548
549 Iglauer, S., Al-Yaseri, A. Z., Rezaee, R., & Lebedev, M. (2015)a. CO₂ wettability of caprocks: Implications for
550 structural storage capacity and containment security. *Geophysical Research Letters*, 42(21), 9279-9284, doi:
551 10.1002/2015GL065787
552
553 Iglauer, S., Pentland, C. H., & Busch, A. (2015)b. CO₂ wettability of seal and reservoir rocks and the implications
554 for carbon geo-sequestration. *Water Resources Research*, 51(1), 729-774, doi: 10.1002/2014WR015553
555
556 Iglauer, S., Salamah, A., Sarmadivaleh, M., Liu, K., & Phan, C. (2014). Contamination of silica surfaces: impact
557 on water-CO₂-quartz and glass contact angle measurements. *International Journal of Greenhouse Gas*
558 *Control*, 22, 325-328, doi: 10.1016/j.ijggc.2014.01.006
559
560 Iglauer, S., Paluszny, A., Pentland, C. H., & Blunt, M. J. (2011)a. Residual CO₂ imaged with X-ray micro-
561 tomography. *Geophysical Research Letters*, 38 (21), doi: 10.1029/2011GL049680
562
563 Iglauer, S., Wüilling, W., Pentland, C. H., Al-Mansoori, S. K., & Blunt, M. J. (2011)b. Capillary-trapping capacity
564 of sandstones and sandpacks. *SPE Journal*, 16(4), 778-783, doi: 10.2118/120960-PA

565 Iglauer, S. (2011)c. Dissolution trapping of carbon dioxide in reservoir formation brine - a carbon storage
566 mechanism. INTECH Open Access Publisher.
567

568 Intergovernmental Panel on Climate Change (IPCC) (2005), IPCC Special Report on Carbon Dioxide Capture
569 and Storage. Prepared by Working Group III of the Intergovernmental Panel on Climate Change, edited by B.
570 Metz et al., Cambridge Univ. Press, Cambridge, United Kingdom, and New York, USA
571

572 Jardine, P. M., McCarthy, J. F., & Weber, N. L. (1989). Mechanisms of dissolved organic carbon adsorption on
573 soil. *Soil Science Society of America Journal*, 53(5), 1378-1385, doi:
574 10.2136/sssaj1989.03615995005300050013x
575

576 Ji, X., & Zhu, C. (2015). CO₂ storage in deep saline aquifers. Chapter 10 in *Novel Materials for Carbon Dioxide*
577 *Mitigation Technology*, 299-332, doi: 10.1016/B978-0-444-63259-3.00010-0
578

579 Jones, D. M., Head, I. M., Gray, N. D., Adams, J. J., Rowan, A. K., Aitken, C. M., ... & Oldenburg, T. (2008).
580 Crude-oil biodegradation via methanogenesis in subsurface petroleum reservoirs. *Nature*, 451(7175), 176, doi:
581 10.1038/nature06484
582

583 Juanes, R., MacMinn, C. W., & Szulczewski, M. L. (2010). The footprint of the CO₂ plume during carbon dioxide
584 storage in saline aquifers: storage efficiency for capillary trapping at the basin scale. *Transport in Porous Media*,
585 82(1), 19-30, doi: 10.1007/s11242-009-9420-3
586

587 Karoussi, O., Skovbjerg, L. L., Hassenkam, T., Stipp, S. S., & Hamouda, A. A. (2008). AFM study of calcite
588 surface exposed to stearic and heptanoic acids. *Colloids and Surfaces A: Physicochemical and Engineering*
589 *Aspects*, 325(3), 107-114, doi: 10.1016/j.colsurfa.2008.04.039
590

591 Kharaka, Y. K., Thordsen, J. J., Hovorka, S. D., Nance, H. S., Cole, D. R., Phelps, T. J., & Knauss, K. G. (2009).
592 Potential environmental issues of CO₂ storage in deep saline aquifers: geochemical results from the Frio-I Brine
593 Pilot test, Texas, USA. *Applied Geochemistry*, 24(6), 1106-1112, doi: 10.1016/j.apgeochem.2009.02.010
594

595 Kleber, M., Eusterhues, K., Keiluweit, M., Mikutta, C., Mikutta, R., & Nico, P. S. (2015). Chapter one-mineral-
596 organic associations: formation, properties, and relevance in soil environments. *Advances in agronomy*, 130, 1-
597 140, doi: 10.1016/bs.agron.2014.10.005
598

599 Krevor, S., Pini, R., Zuo, L., & Benson, S. M. (2012). Relative permeability and trapping of CO₂ and water in
600 sandstone rocks at reservoir conditions. *Water Resources Research*, 48(2), doi: 10.1029/2011WR010859
601

602 Kuhn, H., & Möbius, D. (1971). Systems of monomolecular layers—Assembling and physico-chemical
603 behavior. *Angewandte Chemie International Edition*, 10(9), 620-637, doi: 10.1002/anie.197106201
604

605 Lander, L. M., Siewierski, L. M., Brittain, W. J., & Vogler, E. A. (1993). A systematic comparison of contact
606 angle methods. *Langmuir*, 9(8), 2237-2239, doi: 10.1021/la00032a055
607

608 Legens, C., Toulhoat, H., Cuiec, L., Villieras, F., & Palermo, T. (1998, January). Wettability change related to the
609 adsorption of organic acids on calcite: Experimental and ab initio computational studies. In *SPE Annual Technical*
610 *Conference and Exhibition*. Society of Petroleum Engineers, doi: 10.2118/49319-MS
611

612 Love, J. C., Estroff, L. A., Kriebel, J. K., Nuzzo, R. G., & Whitesides, G. M. (2005). Self-assembled monolayers
613 of thiolates on metals as a form of nanotechnology. *Chemical reviews*, 105(4), 1103-1170, doi:
614 10.1021/cr0300789
615

616 Maboudian, R., & Howe, R. T. (1997). Critical review: Adhesion in surface micromechanical structures. *Journal*
617 *of Vacuum Science & Technology B: Microelectronics and Nanometer Structures Processing, Measurement, and*
618 *Phenomena*, 15(1), 1-20, doi: 10.1116/1.589247
619

620 Madsen, L., & Ida, L. (1998). Adsorption of carboxylic acids on reservoir minerals from organic and aqueous
621 phase. *SPE Reservoir Evaluation & Engineering*, 1(01), 47-51, doi: 10.2118/37292-PA
622

623 Mahadevan, J. (2012). Comments on the paper titled “Contact angle measurements of CO₂–water-quartz/calcite
624 systems in the perspective of carbon sequestration”: A case of contamination?. *International Journal of*
625 *Greenhouse Gas Control*, 7, 261-262, doi: 10.1016/j.ijggc.2011.07.001
626

627 Masalmeh, S. K. (2003). The effect of wettability heterogeneity on capillary pressure and relative
628 permeability. *Journal of Petroleum Science and Engineering*, 39(3-4), 399-408, doi: 10.1016/S0920-
629 4105(03)00078-0
630

631 Meredith, W., Kelland, S. J., & Jones, D. M. (2000). Influence of biodegradation on crude oil acidity and
632 carboxylic acid composition. *Organic Geochemistry*, 31(11), 1059-1073, doi: 10.1016/S0146-6380(00)00136-4
633

634 Morrow, N. R. (1970). Physics and thermodynamics of capillary action in porous media. *Industrial & Engineering*
635 *Chemistry*, 62(6), 32-56
636

637 Morrow, N. R. (1976). Capillary pressure correlations for uniformly wetted porous media. *Journal of Canadian*
638 *Petroleum Technology*, 15(04), doi: 10.2118/76-04-05
639

640 Nordbotten, J. M., Celia, M. A., & Bachu, S. (2005). Injection and storage of CO₂ in deep saline aquifers:
641 analytical solution for CO₂ plume evolution during injection. *Transport in Porous media*, 58(3), 339-360, doi:
642 10.1007/s11242-004-0670-9
643

644 Ochs, M., Čosović, B., & Stumm, W. (1994). Coordinative and hydrophobic interaction of humic substances with
645 hydrophilic Al₂O₃ and hydrophobic mercury surfaces. *Geochimica et Cosmochimica Acta*, 58(2), 639-650, doi:
646 10.1016/0016-7037(94)90494-4
647

648 Orr, F. M. (2009). Onshore geologic storage of CO₂. *Science*, 325(5948), 1656-1658, doi:
649 10.1126/science.1175677
650

651 Paterson, L., Boreham, C., Bunch, M., Ennis-King, J., Freifeld, B., Haese, R., ... & Stalker, L. (2011). The
652 CO₂CRC Otway stage 2B residual saturation and dissolution test: test concept, implementation and data
653 collected. Milestone Report to ANLEC.
654

655 Pearce, J. K., Kirste, D. M., Dawson, G. K., Farquhar, S. M., Biddle, D., Golding, S. D., & Rudolph, V. (2015).
656 SO₂ impurity impacts on experimental and simulated CO₂–water–reservoir rock reactions at carbon storage
657 conditions. *Chemical Geology*, 399, 65-86, doi: 10.1016/j.chemgeo.2014.10.028
658

659 Pentland, C. H., El-Maghraby, R., Georgiadis, A., Iglauer, S., & Blunt, M. J. (2011). Immiscible displacements
660 and capillary trapping in CO₂ storage. *Energy Procedia*, 4, 4969-4976, doi: 10.1016/j.egypro.2011.02.467
661

662 Rahman, T., Lebedev, M., Barifcani, A., & Iglauer, S. (2016). Residual trapping of supercritical CO₂ in oil-wet
663 sandstone. *Journal of colloid and interface science*, 469, 63-68, doi: 10.1016/j.jcis.2016.02.020
664

665 Sarmadivaleh, M., Al-Yaseri, A. Z., & Iglauer, S. (2015). Influence of temperature and pressure on quartz–water–
666 CO₂ contact angle and CO₂–water interfacial tension. *Journal of Colloid and Interface Science*, 441, 59-64, doi:
667 10.1016/j.jcis.2014.11.010
668

669 Shafrin, E. G., & Zisman, W. A. (1962). Effect of progressive fluorination of a fatty acid on the wettability of its
670 adsorbed monolayer. *The Journal of Physical Chemistry*, 66(4), 740-748
671

672 ShojaiKaveh, N., Wolf, K. H., Ashrafizadeh, S. N., & Rudolph, E. S. J. (2012). Effect of coal petrology and
673 pressure on wetting properties of wet coal for CO₂ and flue gas storage. *International Journal of Greenhouse Gas*
674 *Control*, 11, S91-S101, doi: 10.1016/j.ijggc.2012.09.009
675

676 ShojaiKaveh, N., Barnhoorn, A., & Wolf, K. H. (2016). Wettability evaluation of silty shale caprocks for CO₂
677 storage. *International Journal of Greenhouse Gas Control*, 49, 425-435, doi: 10.1016/j.ijggc.2016.04.003
678

679 Stalker, L., Varma, S., Van Gent, D., Haworth, J., & Sharma, S. (2013). South West Hub: a carbon capture and
680 storage project. *Australian Journal of Earth Sciences*, 60(1), 45-58, doi: 10.1080/08120099.2013.756830
681

682 Standnes, D. C., & Austad, T. (2003). Wettability alteration in carbonates: Interaction between cationic surfactant
683 and carboxylates as a key factor in wettability alteration from oil-wet to water-wet conditions. *Colloids and*
684 *Surfaces A: Physicochemical and Engineering Aspects*, 216(1), 243-259, doi: 10.1016/S0927-7757(02)00580-0
685

686 Tabrizy, V. A., Denoyel, R., & Hamouda, A. A. (2011). Characterization of wettability alteration of calcite, quartz
687 and kaolinite: Surface energy analysis. *Colloids and Surfaces A: Physicochemical and Engineering*
688 *Aspects*, 384(1), 98-108, doi: 10.1016/j.colsurfa.2011.03.021.

689

690 Thurman E. M. (1985). *Organic geochemistry of natural waters*. Springer Netherlands, (pp. 151-180)
691

692 Ulrich, H. J., Stumm, W., & Cosovic, B. (1988). Adsorption of aliphatic fatty acids on aquatic interfaces.
693 Comparison between two model surfaces: the mercury electrode and δ -Al₂O₃ colloids. *Environmental science &*
694 *technology*, 22(1), 37-41
695

696 Wan, J., Tokunaga, T. K., Ashby, P. D., Kim, Y., Voltolini, M., Gilbert, B., & DePaolo, D. J. (2018). Supercritical
697 CO₂ uptake by nonswelling phyllosilicates. *Proceedings of the National Academy of Sciences*, 201710853, doi:
698 10.1073/pnas.1710853114
699

700 Wang, S., & Tokunaga, T. K. (2015). Capillary pressure–saturation relations for supercritical CO₂ and brine in
701 limestone/dolomite sands: Implications for geologic carbon sequestration in carbonate reservoirs. *Environmental*
702 *science & technology*, 49(12), 7208-7217, doi: 10.1021/acs.est.5b00826
703

704 Watson, J. S., Jones, D. M., Swannell, R. P. J., & Van Duin, A. C. T. (2002). Formation of carboxylic acids during
705 aerobic biodegradation of crude oil and evidence of microbial oxidation of hopanes. *Organic Geochemistry*,
706 33(10), 1153-1169, doi: 10.1016/S0146-6380(02)00086-4
707

708 White, C. M., Strazisar, B. R., Granite, E. J., Hoffman, J. S., & Pennline, H. W. (2003). Separation and capture of
709 CO₂ from large stationary sources and sequestration in geological formations—coalbeds and deep saline
710 aquifers. *Journal of the Air & Waste Management Association*, 53(6), 645-715, doi:
711 10.1080/10473289.2003.10466206
712

713 Yang, L., Xu, T., Wei, M., Feng, G., Wang, F., & Wang, K. (2015). Dissolution of arkose in dilute acetic acid
714 solution under conditions relevant to burial diagenesis. *Applied Geochemistry*, 54, 65-73, doi:
715 10.1016/j.apgeochem.2015.01.007
716

717 Zasadzinski J. A., Viswanathan R., Madsen L., Garnaes J., & Schwartz D. K. (1994). Langmuir-Blodgett films,
718 *Science (Washington, D.C.)*, 263, 1726 – 1733
719

720 Zullig, J. J., & Morse, J. W. (1988). Interaction of organic acids with carbonate mineral surfaces in seawater and
721 related solutions: I. Fatty acid adsorption. *Geochimica et Cosmochimica Acta*, 52(6), 1667-1678, doi:
722 10.1016/0016-7037(88)90235-9
723